Bioorganic & Medicinal Chemistry xxx (2017) xxx–xxx

Contents lists available at ScienceDirect

Bioorganic & Medicinal Chemistry

journal homepage: www.elsevier.com/locate/bmc

Synthesis and biological activity of novel *tert*-amylphenoxyalkyl (homo) piperidine derivatives as histamine H_3R ligands

Kamil J. Kuder [a], Dorota Łażewska [a], Maria Kaleta [a], Gniewomir Latacz [a], Tim Kottke [b], Agnieszka Olejarz [a], Tadeusz Karcz [a], Andrzej Fruziński [c], Katarzyna Szczepańska [a], Janina Karolak-Wojciechowska [c], Holger Stark [d], Katarzyna Kieć-Kononowicz [a,*]

[a] Department of Technology and Biotechnology of Drugs, Faculty of Pharmacy, Jagiellonian University Medical College, Medyczna 9, Kraków 30-688, Poland
[b] Institute of Pharmaceutical Chemistry, Biozentrun, ZAFES, Frankfurt/Main 60438, Germany
[c] Institute of General and Ecological Chemistry, Technical University of Łódź, Żeromskiego 116 str., Łódź 90-924, Poland
[d] Institute of Pharmaceutical and Medicinal Chemistry, Heinrich-Heine-University, Universitaetsstr. 1, Düsseldorf 40225, Germany

ARTICLE INFO

Article history:
Received 15 December 2016
Revised 13 March 2017
Accepted 15 March 2017
Available online xxxx

Keywords:
Histamine H_3 receptor
Histamine H_3 receptor ligands
Non-imidazole histamine H_3R ligands
Piperidine derivatives
Anticonvulsants
Molecular docking
Drug-like properties

ABSTRACT

As a continuation of our search for novel histamine H_3 receptor ligands a series of twenty new *tert*-amyl phenoxyalkylamine derivatives (**2**–**21**) was synthesized. Compounds of four to eight carbon atoms spacer alkyl chain were evaluated on their binding properties at human histamine H_3 receptor (hH_3R). The highest affinities were observed for pentyl derivatives **6**–**8** (K_i = 8.8–23.4 nM range) and among them piperidine derivative **6** with K_i = 8.8 nM. Structures **6**, **7** were also classified as antagonists in cAMP accumulation assay (with EC_{50} = 157 and 164 nM, respectively). Moreover, new compounds were also evaluated for anticonvulsant activity in Antiepileptic Screening Program (ASP) at National Institute of Neurological Disorders and Stroke (USA). Seven compounds (**2**–**4**, **9**, **11**, **12** and **20**) showed anticonvulsant activity at maximal electroshock (MES) test in the dose of 30 mg/kg at 0.5 h. In the subcutaneous pentetrazole (scMET) test compound **4** showed protection at 100 and 300 mg/kg dose at mice, however compounds showed high neurotoxicity in rotarod test at used doses. Also, molecular modeling studies were undertaken, to explain affinity of compounds at hH_3R (taking into the consideration X-ray analysis of compound **18**). In order to estimate "drug-likeness" of selected compounds *in silico* and experimental evaluation of lipophilicity, metabolic stability and cytotoxicity was performed.

© 2017 Published by Elsevier Ltd.

1. Introduction

Histamine mediates its action through four histamine receptors, that belong to the G-protein coupled receptors superfamily (GPCRs).[1] While histamine H_1 and H_4 receptors are mainly involved in inflammatory processes and response, histamine H_2 receptors mediate the gastric acid secretion, histamine H_3 receptors (H_3R) are involved in the central and peripheral regulation of histamine levels.[2,3] Also, by postsynaptic modulation (as heteroreceptors) they regulate the levels of other neurotransmitters such as acetylcholine, serotonin, noradrenaline, glutamate, γ-aminobutyric acid and neuropeptide Y.[4,5] Therefore, blockade of these "multifunctional" receptors might provide useful pharmacological target in the treatment of many CNS-based diseases. This assumption has been proved by intensive pharmacological studies confirming the utility of histamine H_3R antagonists/inverse agonists in the treatment of Alzheimer and Parkinson's diseases, schizophrenia, narcolepsy, obesity and attention-deficit hyperactivity disorder (ADHD).[6,7] Dual- and multi target acting ligands addressing, apart of H_3R, various therapeutic targets have also been described.[8–10] Among a number of active compounds obtained in both academia and industry,[11,12] only one histamine H_3R antagonist, *Pitolisant* (Bioprojet Biotech) completed phase III of clinical trials with positive results in narcolepsy and daytime sleepiness in Parkinson's disease,[13] and is accepted by European Medicines Agency as an orphan drug under the name of *Wakix* (Pitolisant hydrochloride) by Bioprojet Pharma.[14] However, safety pharmacology studies highlighted the ability of Pitolisant to affect the QT interval in humans, as well as its pro-convulsant potential, The European Medicines Agency's Committee for Medicinal Products for Human

* Corresponding author.
E-mail address: mfkonono@cyf-kr.edu.pl (K. Kieć-Kononowicz).

http://dx.doi.org/10.1016/j.bmc.2017.03.031
0968-0896/© 2017 Published by Elsevier Ltd.

Use decided that Wakix's benefits are greater than its risks and recommended that it be approved for use in the EU.

Despite the variety of the structures of active H_3R ligands, all of them fit to the proposed blueprint: basic, mostly cyclic, amine connected by aliphatic (rigidified) linker with polar moiety, connected with arbitrary region, that may contain polar, acidic, basic, lipophilic and even metal-containing substituents.[15] While amine-aliphatic part is mostly responsible for ligand's affinity, the arbitrary region might influence activity and pharmacokinetic properties.[16,17] One must also pay attention to the fact, that at least six H_3R isoforms in the human and more than 20 in other species have been found. A wide variety of such isoforms might result in different brain expression and signaling. Thus binding heterogeneity of ligands might be the result of different splicing variants of the same protein.[18]

Basing on our previous results, as well as on those described in literature, novel structures were designed according to proposed pharmacophore pattern for histamine H_3R ligands. The main aim of this work was to obtain *N*-alkyl(substituted)piperidine ether derivatives with expected histamine H_3R affinity. As a lead structure for further modifications, previously described and obtained in our group compound **DL77**[19,20] has been chosen. Modifications included: ascending alkyl chain length (4–8 methylene groups) as well as modifications of piperidine moiety – un/substituted piperidines, hexamethyleneimine (homopiperidine), in the basic part of compounds (Fig. 1).

2. Results and discussion

2.1. Chemistry

The synthesis of desired ether derivatives **2**–**21** was achieved through the efficient synthetic route outlined in Scheme 1.

Para tert-amylphenoxyalkyl bromides (**1a**–**1e**, synthesis according,[21] modified by authors) were obtained in one-step alkylation of *para tert*-amylphenol with α,ω-dibromoalkanes refluxed in propan-1-ol.[22] Obtained precursor bromides, after the separation from *bis* products, that was created during synthesis, were then coupled with corresponding cycloalkylamines in the mixture of ethanol/water with powdered potassium carbonate and a catalytic amount of potassium iodide. The desired products were obtained as free bases and isolated as oxalic acid salts.

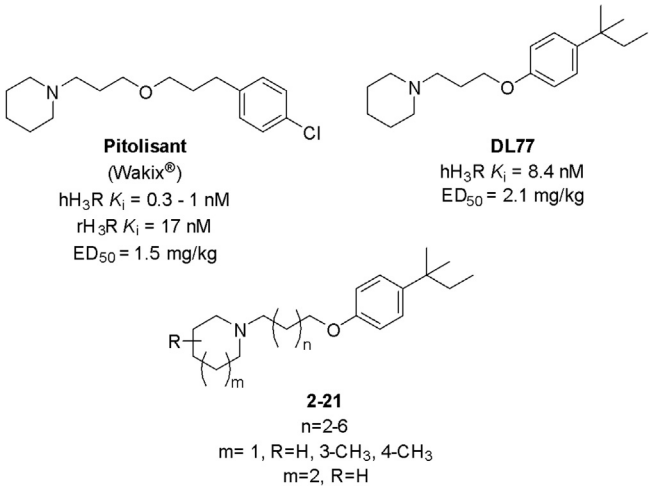

Fig. 1. Pitolisant (Wakix® – top left),[13] DL77(top right)[18] and general structure of described ligands **2**–**21** (bottom); hH_3R – human histamine H_3 receptor; rH_3R – rat histamine H_3R.

2.2. Pharmacology

2.2.1. Histamine H_3 receptor affinity

All compounds in their oxalate forms were then presented for histamine H_3R *in vitro* binding studies, as described by Ligneau et al.[23] and Kottke et al.[24] [^{125}I]Iodoproxyfan or [^{3}H]N^{α}-methylhistamine were used as the radioligands in binding assays to test the affinity at human recombinant histamine H_3R stably expressed in CHO-K1[23] cells or human embryonic kidney (HEK-293) cells.[24]

Pharmacological results are assembled in Table 1. All of the compounds showed good to very good affinities for human H_3R (hH_3R) in K_i range of 8–325 nM.

In 1992 Lipp and co-workers[25] proposed the general pharmacophore for histamine H_3R antagonists, where nitrogen containing ring is connected via aliphatic linker with polar moiety. Customarily, the length of such linker is 3 methylene groups. One of the first to describe active ligands with longer linker consisted of 3–6 methylene groups was Ganellin et al. in 1998,[26] where the *in vitro* affinity of the compounds was of high values (hH_3R K_i = 0.019–0.46 μM) independently of the linker length (3–5 methylene groups alkyl spacer).

In this work we focused on compounds with elongated alkyl chain (4–8 methylene groups), derived from previously described, high potent compound **DL77** (hH_3R K_i = 8.4 nM; ED_{50} = 2.1 mg/kg) described by Łażewska et al.[19] For the series of presented ligands, one can observe that the *in vitro* affinity to H_3R decreases with the elongation of the linker. However, compounds of 4 methylene linker group whose activity is placed in-between the group of 7 and 8 methylene linker groups, are still on high level (K_i = 46–238 nM), they seem to be an exception to this rule. Compounds with 5 methylene linker (**6**–**9**) were the most active group (K_i 8.8–23.4 nM). For each of the presented subgroups, 3-methylpiperidine derivatives show the highest affinity to H_3R (e.g. compounds: **3**, **11**, **15**, **19**), with, again, the exception of compound **7**, that has slightly lower affinity than its piperidine homologue **6** – the most active compound of herein described series (hH_3R K_i = 8.8 nM). In fact compound **6** retained the affinity of reference compound – **DL77**. Oppositely, the lowest affinities in the subgroups show the 4-methylpiperidine derivatives, with the exception of previously mentioned subgroups of 7 and 8 methylene long linker, where homopiperidine derivatives were of lowest hH_3R affinity (eg. compound **16** vs. **17** and **20** vs. **21**).

Paying attention to the overall high affinity of the obtained compounds, it can be assumed, that the linker length, and various piperidine derivatives determines their affinity for histamine H_3R.

2.2.2. Functional properties at histamine H_3 receptor

Selected, most potent structures (**6** and **7**) were further investigated in functional tests in order to determine their intrinsic activity. For that purpose cAMP accumulation assay at HEK293 cells expressing recombinant human histamine H_3R was employed. Investigated compounds caused a blockade of cAMP level reduction by receptor agonist, in cells co-treated with forskolin (H_3R is a G_i-coupled receptor) and were therefore classified as histamine H_3R antagonists. Antagonist potency (EC_{50}) was evaluated by performing a dose-response curve experiment in presence of H_3R agonist – (*R*)(−)-α-methylhistamine (15 nM, corresponding to its EC_{80}) and forskolin (10 μM) (Fig. 2). Obtained EC_{50} values were as follows: **6** – EC_{50} = 157 ± 16 nM; **7** – EC_{50} = 164 ± 37 nM (Fig. 2).

2.2.3. Anticonvulsant activity

Given H_3R localization and their ability to influence multiple neurotransmitter systems (eg. glutamate, GABA), targeting central H_3R's might find its use in epilepsy treatment. Therefore, selected (16) compounds were screened *in vivo* for anticonvulsant activity.

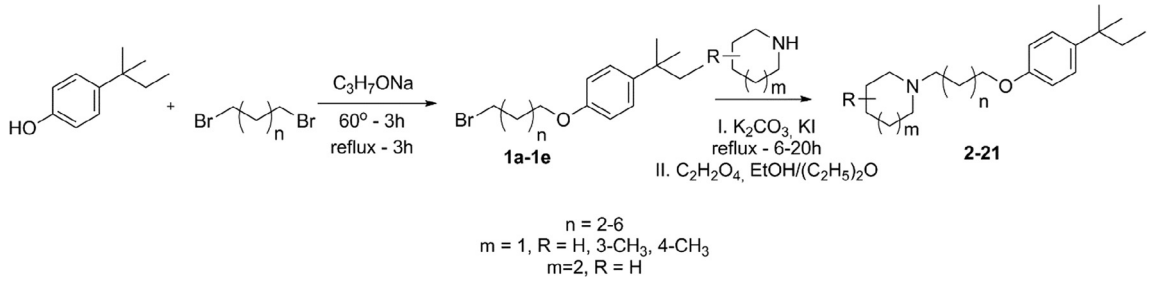

Scheme 1. General synthetic pathway for compounds **2**–**21**.

Table 1
Structures of compounds **2**–**21** and their pharmacological *in vitro* properties.

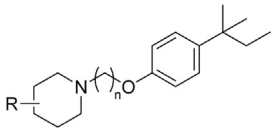

No.	n	R	hH_3R K_i [nM]	No.	n	R	hH_3R K_i [nM]
DL77	3	–	8.4 ± 1.3[a]	**12**	6	4-CH_3	60.5[d]
2	4	–	140 ± 47[b,c]	**13**	6	–CH_2–	41.2[d]
3	4	3-CH_3	46 ± 22[b]	**14**	7	–	55[c,d]
4	4	4-CH_3	238 ± 95[b]	**15**	7	3-CH_3	36.6[d]
5	4	–CH_2–	68 ± 20[b]	**16**	7	4-CH_3	64.4[d]
6	5	–	8.8[c,d]	**17**	7	–CH_2–	128.3[d]
7	5	3-CH_3	13.6[d]	**18**	8	–	325.9[d]
8	5	4-CH_3	23.4[d]	**19**	8	3-CH_3	120.7[d]
9	5	–CH_2–	21.4[c,d]	**20**	8	4-CH_3	308.1[d]
10	6	–	46.5[c,d]	**21**	8	–CH_2–	182.5[d]
11	6	3-CH_3	33.8[d]				

[a] Data from Ref. 18.
[b] [^{3}H] N^{α}Methylhistamine as radioligand, mean values ± SD, as described by Kottke et al.[24].
[c] Histamine hH_3R affinity has been previously shown by Sadek et al.[20].
[d] [^{125}I] Iodoproxyfan binding to membranes of CHO-K1 cells expressing human H_3R as described by Ligneau et al.,[23] data from a single experiment with each concentrations tested at least in triplicate.

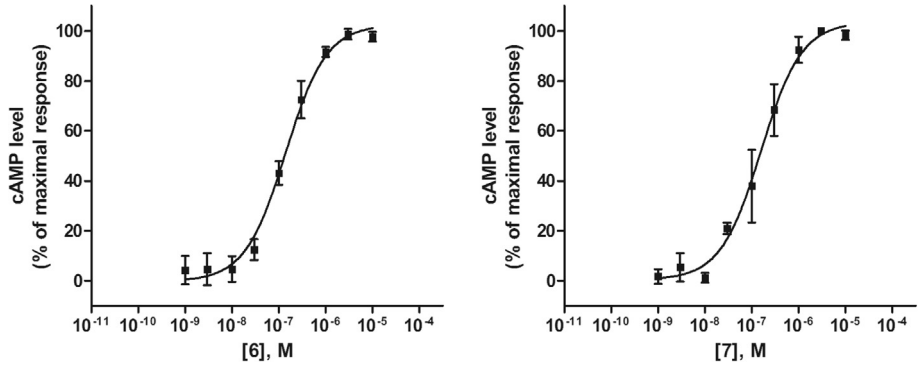

Fig. 2. cAMP accumulation studies in HEK293 cells expressing the human histamine H_3 receptor, co-treated with forskolin, (*R*)(−)-α-methylhistamine and tested compounds: **6** (left) and **7** (right).

All tests were carried out at National Institute of Neurological Disorders and Stroke, National Institutes of Health (Rockville, USA) within Anticonvulsant Screening Program (ASP) according to known, standardized procedures.[27,28] Sixteen compounds (**2**–**7**, **9**–**16**, **19**, **20**) were subjected to standard protocols including three tests: the maximal electroshock (MES), subcutaneous pentetrazole for anticonvulsant activity (scMET) and rotarod test (TOX) for neurotoxicity. Tests were performed in mice at 0.5 h and 4 h after intraperitoneal (i.p.) administration of the studied compounds. Results of the anticonvulsant screening are presented in Table 2. Seven compounds (**2**–**4**, **9**, **11**, **12**, and **20**) showed anticonvulsant activity tested in the dose of 30 mg/kg at 0.5 h. All tested compounds were active at the dose of 100 mg/kg at 0.5 h after administration, while twelve of them (**2**, **3**, **5**, **7**, **9**, **10**–**12**, **15**, **16**, **19** and **20**) were also active up to 4 h after administration. One compound (4-methyl piperidinyl hexyl derivative **12**) proved to be active in the MES at the dose of 30 and 100 mg/kg up to 4 h of tested time. All compounds showed high toxicity in the active dose, and caused the death of all animals. In the scMET study only 4-methyl piperidine derivative **4** with butyl chain showed protection at 100 and

Table 2
Preliminary anticonvulsant evaluation of compounds **2**–**20** in the MES, scMET and TOX test (mice, i.p.).*

Com	Dose [mg/kg]	MES[1]		scMET[2]		TOX[3]	
		0.5 h	4.0 h	0.5 h	4.0 h	0.5 h	4.0 h
2	30	**1/1**	0/1	0/1	0/1	**2/4**	0/2
	100	**3/3**	**2/3**	0/1	0/1	**8/8**[a]	0/4
	300	**–**	**–**	–	–	**4/4**[b]	–
3	30	**1/1**	0/1	0/1	0/1	**3/4**	0/2
	100	**3/3**	**1/1**	–	0/1	**8/8**[a]	**4/4**[b]
	300	**–**	**–**	**–**	–	**4/4**[b]	**–**
4	30	**1/1**	0/1	0/1	0/1	**1/4**	0/2
	100	**3/3**	0/3	**1/1**	–	**8/8**[b]	–
	300	**–**	–	**1/1**	**–**	**4/4**[b,c,d]	**–**
5	30	0/1	0/1	–	–	**1/4**[b]	0/2
	100	**2/2**	**1/1**	**–**	**–**	**8/8**[b,c]	**1/2**[b]
	300	**–**	**–**	**–**	**–**	**4/4**[b,c]	**–**
6	30	0/1	0/1	0/1	0/1	0/4	0/2
	100	**3/3**	0/3	0/1	0/1	**6/8**[a]	0/4
	300	**–**	–	–	–	**4/4**[b]	–
7	30	0/1	0/1	0/1	0/1	0/4	0/2
	100	**2/3**	**3/3**	0/1	0/1	**7/8**[a]	**1/4**
	300	**–**	**–**	–	–	**4/4**[b]	**–**
8	30–300	nt	nt	nt	nt	nt	nt
9	30	**1/1**	0/1	0/1	0/1	0/4	**0/2**
	100	**3/3**	**1/2**	0/1	0/1	**6/8**[a,e,f]	**3/4**[b]
	300	**–**	–	–	–	**4/4**[b]	**–**
10	30	0/1	0/1	0/1	0/1	0/4	0/2
	100	**3/3**	**3/3**	0/1	0/1	**7/8**	0/4
	300	**–**	**–**	–	–	**4/4**[a,b]	–
11	30	**1/1**	0/1	0/1	0/1	0/4	0/2
	100	**3/3**	**3/3**	0/1	0/1	**8/8**[g]	**3/4**
	300	**1/1**	–	–	–	**4/4**[b,d]	–
12	30	**1/1**	**1/1**	0/1	0/1	0/4	0/2
	100	**3/3**	**3/3**	0/1	0/1	**6/8**[a]	**3/4**
	300	**1/1**	**–**	–	–	**4/4**[b]	**–**
13	30	0/1	0/1	0/1	0/1	0/4	0/2
	100	**3/3**	0/3	0/1	0/1	**8/8**[a]	**3/4**
	300	**–**	–	–	–	**4/4**[b]	**–**
14	30	0/1	0/1	0/1	0/1	0/4	0/2
	100	**3/3**	0/3	0/1	0/1	**7/8**[a]	0/4
	300	**1/1**	–	–	–	**4/4**[a,b]	0/1
15	30	0/1	0/1	0/1	0/1	0/4	0/2
	100	**2/3**	**3/3**	0/1	0/1	**6/8**	**2/4**
	300	**1/1**	0/1	0/1		**3/4**	**1/2**[b]
16	30	0/1	0/1	0/1	0/1	0/4	0/2
	100	**3/3**	**3/3**	0/1	0/1	**7/8**[a]	**3/4**[a]
	300	**–**	**–**	–	–	**4/4**[b]	**–**
17	30–300	nt	nt	nt	nt	nt	nt
18	30–300	nt	nt	nt	nt	nt	nt
19	30	0/1	0/1	0/1	0/1	0/4	0/2
	100	**1/3**	**3/3**	0/1	0/1	**1/8**	0/4
	300	**1/1**	**–**	0/1	0/1	**2/4**	**2/2**[b]
20	30	**1/1**	0/1	0/1	0/1	**1/4**	0/2
	100	**1/3**	**2/2**	0/1	0/1	**8/8**	**4/4**[b]
	300	**1/1**	**–**	0/1	0/1	**4/4**[a,b]	**1/1**[b]
21	30–300	nt	nt	nt	nt	nt	nt

nt – not tested – the compound was not tested in the particular case.
[a–g]Kind of toxicity: [a]unable to grasp rotorod; [b]death; [c]diarrhea; [d]continuous seizure activity; [e]loss of righting reflex; [f]myoclonic jerks; [g]tremors.
* Ratios where at least one animal was protected have been highlighted in bold for easier data interpretation.
[1] MES – maximum electroshock seizure: number of animals protected/number of animals tested.
[2] scMet – subcutaneous pentetrazole evoked seizure test: number of animals protected/number of animals tested.
[3] TOX – neurotoxicity assay (the rotarod test): number of animals exhibiting toxicity/number of animals tested.

300 mg/kg, but these doses caused also severe toxicity. Three compounds (**2**, **3**, and **19**) were also tested in MES after oral administration to rats (30 mg/kg) but they did not show any activity (data not shown).

2.3. Physicochemical properties

2.3.1. Lipophilicity evaluation

As physicochemical properties might determine the fate of novel compounds, at the early stage of research, their lipophilicity was evaluated using planar RP-TLC method and expressed by R_{M0} values.[29] Ternary solvent mixture – methanol:acetic acid:water – as the mobile phase was used, with constant, 10% concentration of acetic acid and varying methanol concentration in the range of 50–80%. Due to high similarity of 3- and 4-methylpiperidine isomers, lipophilicity was estimated only for 3-methylpiperidine derivatives. Tested set of compounds showed R_{M0} values in range between 1.883 and 3.562. All of the values are over 2 (except compound **2**), which may suggest good biological barriers permeability. Lipophilicity studies data are collected in Table 3. Sample graph, showing the relationship between R_{M0} values and methanol concentration for compound **18** is shown in Fig. 3. As it was expected,

lipophilicity of the tested set of compounds rises with the elongation of the alkyl chain length. Moreover, for structural analogues (3-methylpiperidine and azepane derivatives) values resulted in the similar range, e.g. compounds **11** and **13**, **15** and **17**. Although, no correlation between lipophilicity and hH_3R affinity was observed for the tested series.

In order to compare the theoretical partition coefficient parameters (logP) with ones obtained practically, calculations using computer programs: Chem3D,[30] Marvin[31] and QikProp for Schrödinger[32] were also performed. All of the compounds were used in both: base and ionic forms. The latter obtained theoretical values seem to be more realistic, due to the fact, that all of the tested compounds are hydrogen oxalates. The values vary between programs, due to various algorithms used by software to determine lipophilicity values. The highest theoretical to practical values ratio was obtained using Marvin software (R = 0.92158, R^2 = 0.84931). Correlation coefficient (R), regression line slope (a), standard deviation (SD) and R^2 values are collected in Table 3.

2.3.2. In silico solubility estimation

As low aqueous solubility of compounds might be the major problem encountered with development of new chemical entities, by affecting e.g. absorption and distribution, thus, activity towards desired biological target, conformation independent (CI) solubility factor, by means of logS [mol/dm^3] was calculated for the series of compounds, using QikProp 3.2 for Schrödinger[32] (Table 3). For all of the compounds the predicted solubility is moderate (with lowest value for compound **9**), although still in the characteristic range for market drugs. Also, no correlation between logS values and hH_3R affinity was observed for the tested series.

2.4. X-ray studies and in silico molecular and Docking studies

Monocrystal of compound **18** (in the hydrogen oxalate form) was selected as suitable for X-ray structure analysis. The structure was solved in non-centrosymmetric triclinic space group *P*1 with two independent molecules. Both molecules adopt extended conformation with proton located at nitrogen (Fig. 4). Independent molecules differ in C7-C8-C9-C10-C11-C12-C13-C14 chain conformation details and *tert*-pentyl rotation. In the crystals main protonated molecules are twisted around the oxalate ions chain. For detailed information see Appendix A. Supplementary Materials.

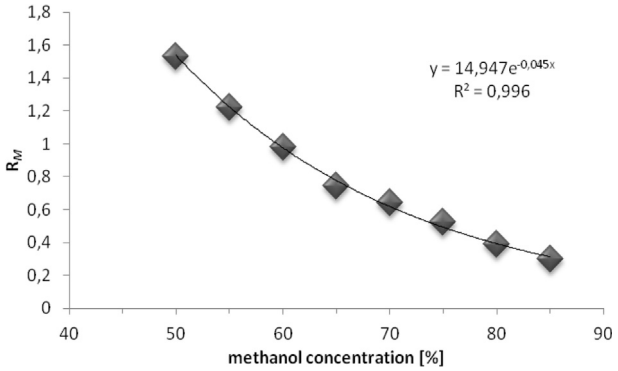

Fig. 3. Relationship between R_{M0} values and methanol concentration for compound **18**.

Computational approaches, using Schrödinger Maestro 10.5.014,[32] allowed the *in silico* binding visualization of the investigated compounds to histamine H_3R homology model obtained from GPCRM Structure Modeling Server.[33] The model was built on the crystal structure of M_3 muscarinic acetylcholine receptor, due to its' highest sequence homology to histamine H_3R aminoacid sequence (PDB code: 4DAJ; resolution: 3.4 Å). Validation with reference ligand *Pitolisant*, according to the procedure described by Levoin et al. was also performed.[34] Docking studies results were interpreted by the means of Docking Score function values, that resulted in the range of −9.001 (**17**) to −6.398 (**21**). Previously described salt bridge formation between the protonated cycloalkylamine nitrogen and GLU206$^{5.461}$,[35] described as crucial for H_3R antagonist/inverse agonist binding, [36] could be observed for all of the compounds regardless of their *in vitro* affinity (Fig. 5, Table 1). Moreover, for all of the ligands π–π stacking could be observed between PHE198$^{5.39}$ and/or TYR189(ECL2) and substituted benzene ring of docked compounds. Moreover, for compounds of longer (6–8 methylene groups) alkyl chain length, additional π–π stacking with TYR115$^{3.33}$ was observed. This phenomenon was likewise observed for the reference compound **DL77**.

None of the compounds showed previously described interaction between ether moiety oxygen and TYR374$^{6.51}$, although π–π stacking with substituted phenyl ring was observed. What was interesting, for methylated piperidine derivatives, which are of higher *in vitro* affinity than non-methylated ones, none additional

Table 3
Theoretical and practical lipophilicity and solubility (CI logS) values for compounds **2**–**21**, as well as R, R^2, a and SD values for each of the used computational programs.

No	R_{M0}	Marvin 5.4.1.1		ChemBio3D Ultra 11.0		QikProp 3.2	CI logS
		Ionic	Base	Ionic	Base	Ionic	
2	1.883	1.75	5.25	6.581	6.161	5.128	−3.590
3	2.294	2.12	5.62	7.100	6.680	5.627	−3.888
5	2.292	2.19	5.70	7.140	6.720	5.016	−3.888
6	2.172	2.19	5.70	7.110	6.690	5.451	−3.463
7	2.342	2.56	6.06	7.629	7.209	5.813	−3.888
9	2.389	2.64	6.14	7.669	7.249	5.750	−6.099
10	2.456	2.64	6.14	7.639	7.219	5.853	−4.185
11	2.521	3.00	6.51	8.158	7.738	6.200	−3.761
13	2.567	3.08	6.59	8.198	7.778	5.596	−4.185
14	2.624	3.08	6.59	8.168	7.748	6.240	−4.483
15	2.983	3.45	6.95	8.687	8.267	6.596	−4.483
17	2.926	3.53	7.03	8.727	8.307	6.615	−4.059
18	3.075	3.53	7.03	8.697	8.277	6.570	−4.483
19	3.562	3.89	7.39	9.216	8.796	6.884	−4.781
21	3.384	3.97	7.47	9.256	8.836	7.057	−4.781
R		0.92158	0.92141	0.93709	0.93692	0.91834	
R^2		0.84931	0.84898	0.87815	0.87783	0.84335	
a		0.72523	0.72483	0.77804	0.78491	1.11644	
SD		1.30901	2.19606	2.92496	2.73370	2.11186	

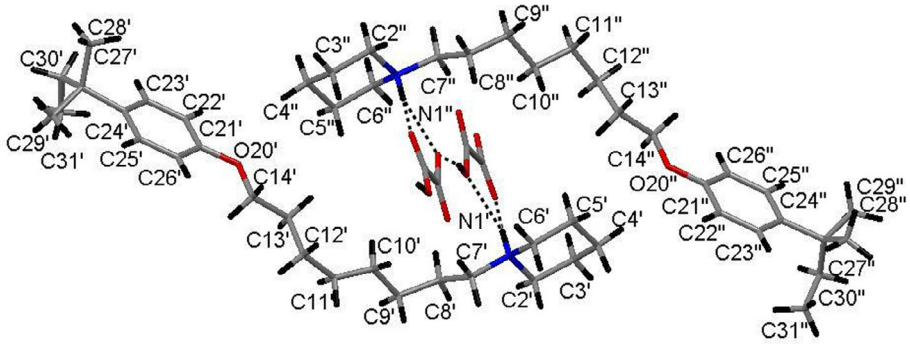

Fig. 4. ORTHEP drawing of **18** hydrogen oxalate structure (light grey color for carbons, red for oxygen, blue for nitrogen).

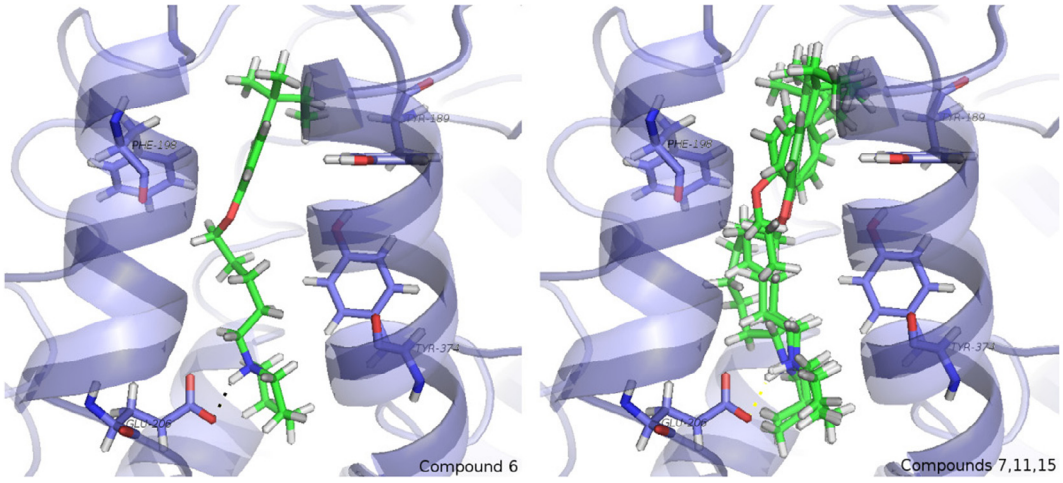

Fig. 5. Compound **6**, and **7**, **11**, **15** in the binging pocket of histamine H_3 receptor homology model (ligands: green color for carbons, white – hydrogens, blue – nitrogen, red – oxygen; receptor – cyan for carbons, white – hydrogens, blue – nitrogen, red – oxygen).

interactions between methyl group and side-chains amino acids were found. Although, nevertheless the spacer length, methylene groups are placed in one position, surrounded by small pocket formed by CYS118$^{3.37}$, THR119$^{3.38}$ and ALA122$^{3.40}$ (Figs. 5 and 6). This interaction might condition higher affinity to H_3R of 3-methylpiperidine derivatives.

2.5. Drug-like properties

The acceptable ADME-Tox parameters of the biologically active compound describe its "drug-likeness" – namely, the ability to become an ideal clinical candidate.[37] Presented in this study, most active H_3R ligands **6**, **7**, **8** and **9** were chosen for examination of two important ADME-Tox parameters: toxicity and metabolic stability.

2.5.1. Toxicity

Toxicity of novel compounds was determined *in vitro* after incubation of HEK-293 cell line in the presence of H_3R ligands for 48 h. Obtained data showed the decreasing viability of examined cells above the 10 μM concentration with IC_{50} values from 25.1 μM to 41.19 μM (Fig. 7). The highest activity against HEK-293 cell line was shown for compound **7**, the derivative with the methyl substituent at 2-position of piperidine moiety (Fig. 7). However, observed antiproliferative effects of examined compounds could be described as weak, being 50–90-fold lower in comparison to IC_{50} value of the reference compound doxorubicin (DX) (0.46 μM).[38] On the other hand, antiproliferative assays have found its way to be useful tools in drug discovery and development of new anticancer therapeutics.[39] Therefore, the additional tests were performed with neuroblastoma IMR-32 cell line, where compounds **7**, **8**, **9** showed similar activity against IMR-32. The highest activity in these tests showed compound **9**, the derivative with azepane moiety, with IC_{50} = 12.31 μM. However, significant effect of **9** against IMR-32 was observed under more than 1000-fold higher concentration in comparison to IC_{50} value of the reference compound DX, which was found to be only 5.1 nM. (Fig. 8).

2.5.2. Metabolic stability

In first instance, compounds **6**, **7**, **8** and **9** were examined *in silico* using MetaSite 4.1.1software,[40] to predict the most likely sites of metabolic transformations. The highest probability of metabolism calculated by liver model for compounds **7**, **8** occurred at 3- and 4-substituted position of piperidine moiety, whereas for compounds **6** and **9** MetaSite predicted the highest possibility of metabolism at the aliphatic linker. For all of the compounds the possibility of hydroxylation of *tert*-amyl moiety was also considered. The locations of metabolic modifications are shown in Fig. 9.

In the next step the examined H_3R ligands were incubated for 2 h with human liver microsomes (HLMs). A full scan chromatogram of the reaction mixtures showed the presence of 3 metabolites for compounds **6**, **7**, **8** and the presence of 5 metabolites for compound **9**. The LC/MS analysis allowed to indentify the molecular masses of obtained metabolites, as well as to confirm the structures of HLMs obtained metabolites, ion fragments analysis was performed. The obtained data showed the

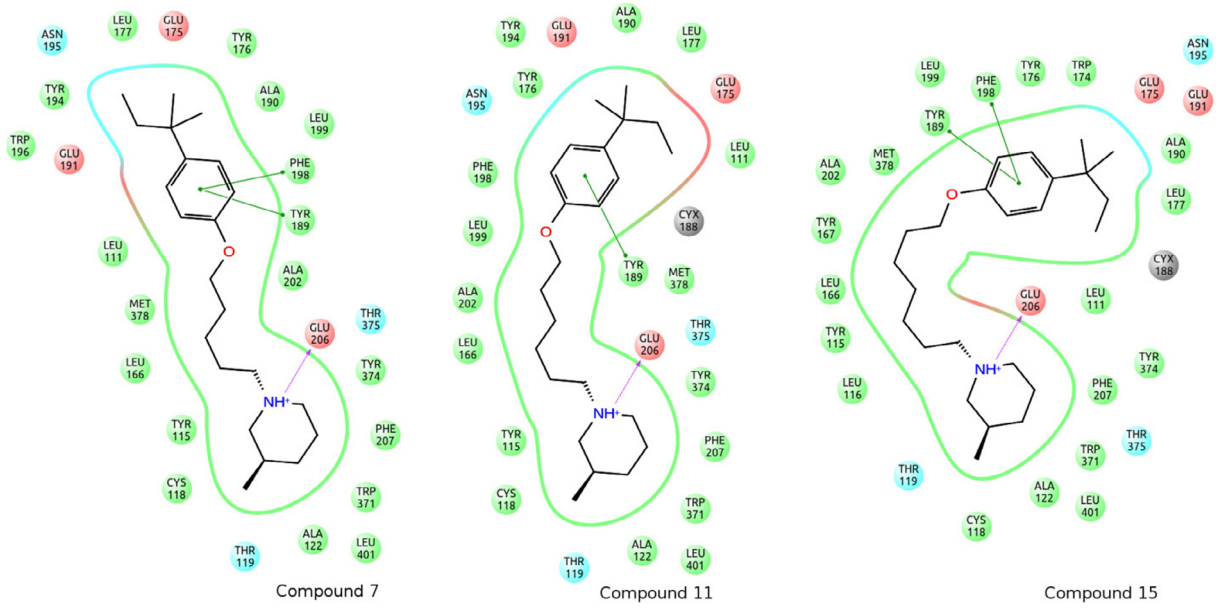

Fig. 6. Ligand – interaction diagrams (generated using Schrödinger Suite) for compounds **7**, **11**, **15**.

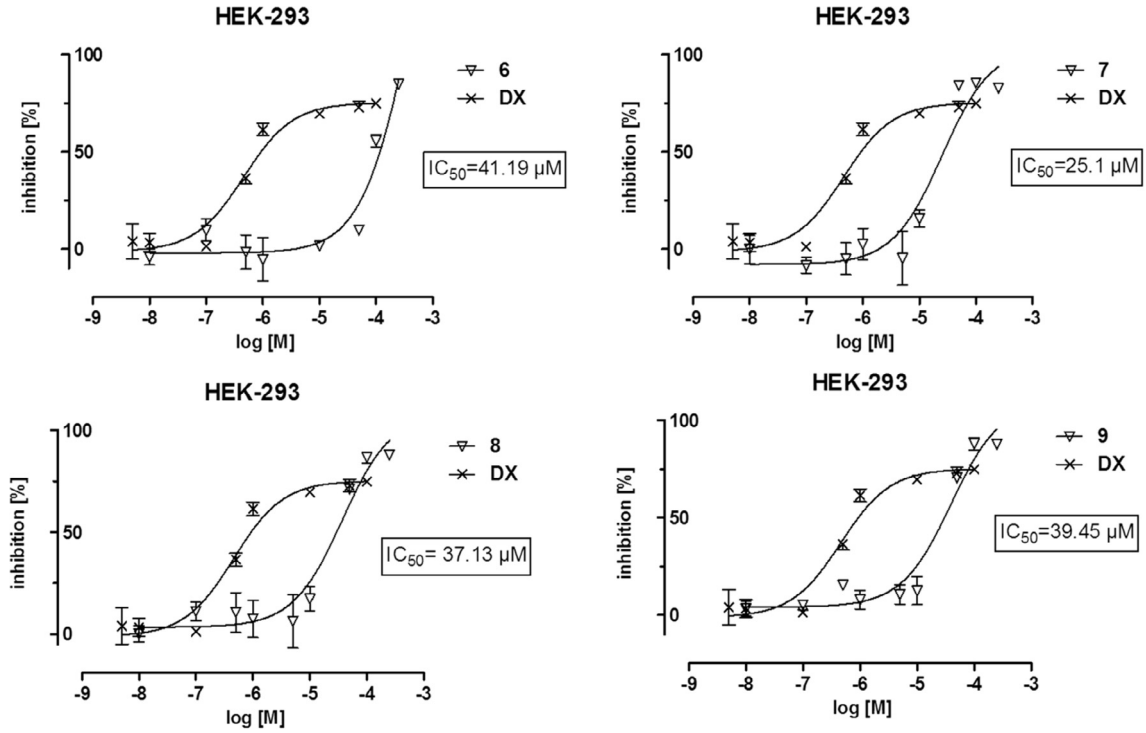

Fig. 7. Activity of DX (positive standard) and H_3 receptor ligands (**6**–**9**) against HEK-293 cell line.

similar metabolism pathway of compounds **6** ($[M+H]^+ = 318$ *m*/*z*), **7** ($[M+H]^+ = 332$ *m*/*z*), and **8** ($[M+H]^+ = 332$ *m*/*z*), where the hydroxylation occurred in three different ways at the *tert*-amyl moiety (metabolites: M1, M2 and M3;see Appendix A). At first, it was observed that the molecular masses of metabolites increased to 334 *m*/*z* compared to substrate **6** or to 348 *m*/*z* compared to substrates **7**, **8**. Moreover, the characteristic for all substrates *tert*-amyl ion fragment (71 *m*/*z*) was absent in the all metabolites spectra and the precise analysis of the another ion fragments excluded the hydroxylation in piperidine moiety or in the aliphatic linker. The metabolic pathway of compound **9** ($[M+H]^+ = 332$ *m*/*z*) included similar to compounds **6**, **7** and **8** reactions of hydroxylation at *tert*-amyl moiety (metabolites M2, M3 and M4) and additional two metabolites M1 and M5. The additional metabolite M1 ($[M+H]^+ = 320$ *m*/*z*) is probably the product of demethylation followed by hydroxylation. The molecular mass of second additional metabolite M5 ($[M+H]^+ = 364$ *m*/*z*) suggested the double hydroxylation of the substrate. The presence of characteristic *tert*-amyl ion fragment 71 *m*/*z* excluded the hydroxylation of *tert*-amyl moiety. The precise study of ion fragments of M5 showed that the hydroxylation occurred at the azepane moiety and at the methylene bridge connected to nitrogen in the azepane moiety.

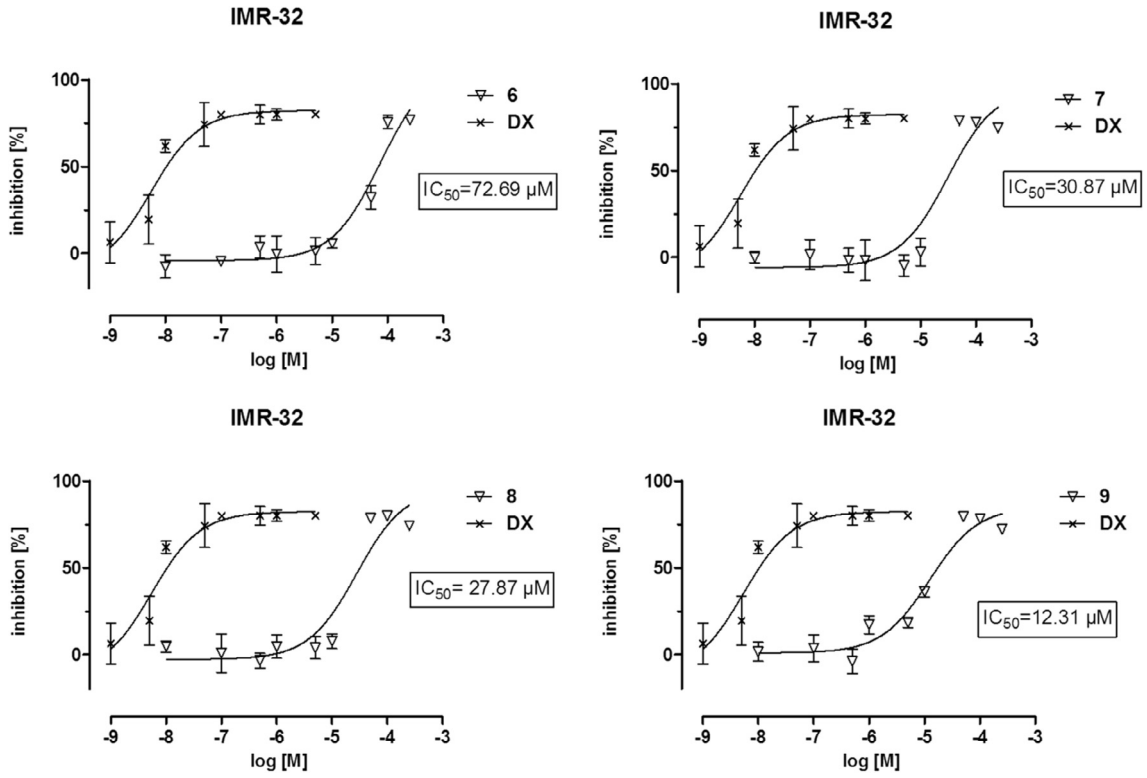

Fig. 8. Activity of DX (positive standard) and H_3 receptor ligands (**6**–**9**) against IMR-32 cell line.

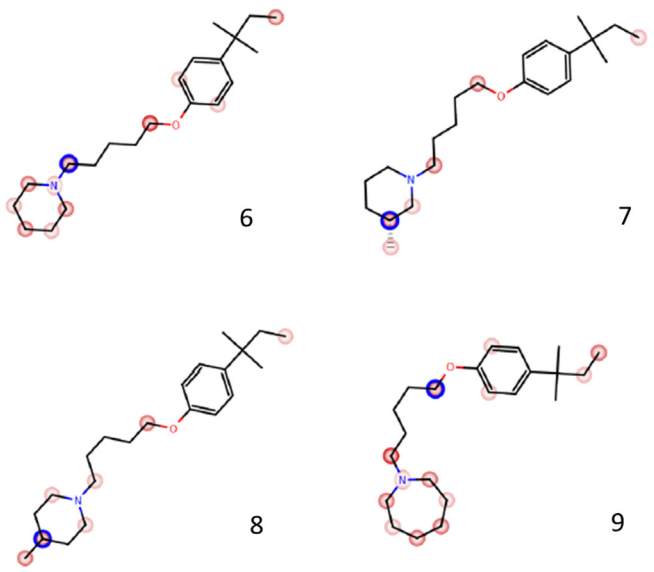

Fig. 9. Plots of MetaSite predictions for sites of metabolism for H_3 receptor ligands by liver model. Higher color intensity of the marked functional group indicates higher probability of its involvement in the metabolism pathway. The blue circle indicates the highest probability to be involved in the metabolism pathway.

2.5.3. Influence on cytochrome CYP3A4 activity

The luminescence CYP3A4 P450-Glo™ Assay based on the conversion of the luciferin-PPXE into D-luciferin by recombinant human CYP3A4 was next used to determine the influence of examined H_3R ligands on cytochrome CYP3A4 activity. After addition of the firefly luciferase, the measured amount of light produced was proportional to D-luciferin concentration and allowed to assess the effect of examined compound on CYP3A4.[41] In that assay, the reference compound ketoconazole inhibited completely the CYP3A4 activity at 10 μM with calculated IC_{50} = 0.14 μM.[42] Depending on the structure of the H_3R ligand, weak or very strong activations of CYP3A4 were observed. In the presence of 25 μM of compound **8** with the methyl substituent at the 4-position of piperidine moiety, the CYP3A4 activity increased surprisingly by 325%. However, compound **7** with the same substituent at the 3-position increased the cytochrome activity only by 52% at 25 μM, similar to compound **9** with azepane moiety (76%). The weakest influence on CYP3A4 showed compound **6** with unsubstituted piperidine moiety, which increased the cytochrome activity only by 21% at 25 μM (Fig. 10).

3. Conclusions

A novel series of *tert*-amyl phenoxy alkylamine derivatives investigated in the present study proved to be potent histamine H_3R ligands with the H_3R affinities in the nanomolar range. The highest affinities were observed for pentyl derivatives **6** and **7** (K_i = 8.8 and 13.6 nM, respectively) with piperidine and 3-methyl piperidine cycloalkylamines. The length of alkyl chain and character of amine have pronounced effect on the activity – generally, for this group, 3-methyl piperidine derivative with five carbon atoms chain was the most potent. Further elongation of the alkyl linker resulted in decrement of H_3R affinity. Selected, representative structures were described as antagonists in cAMP test. Performed *in vivo* studies proved anticonvulsant activity in MES test for all of the examined compounds. On the other hand, only one compound has shown the activity in scMET test. Docking studies to histamine H_3R homology model built on the crystal structure of M_3 muscarinic acetylcholine receptor allowed the observation of previously proposed ligand-receptor interactions. Experimentally estimated lipophilic properties (by means of R_{M0}) may suggest good tissues barriers permeability. Moreover, the examined compounds show satisfying, selected (cytotoxicity, metabolic stability, influ-

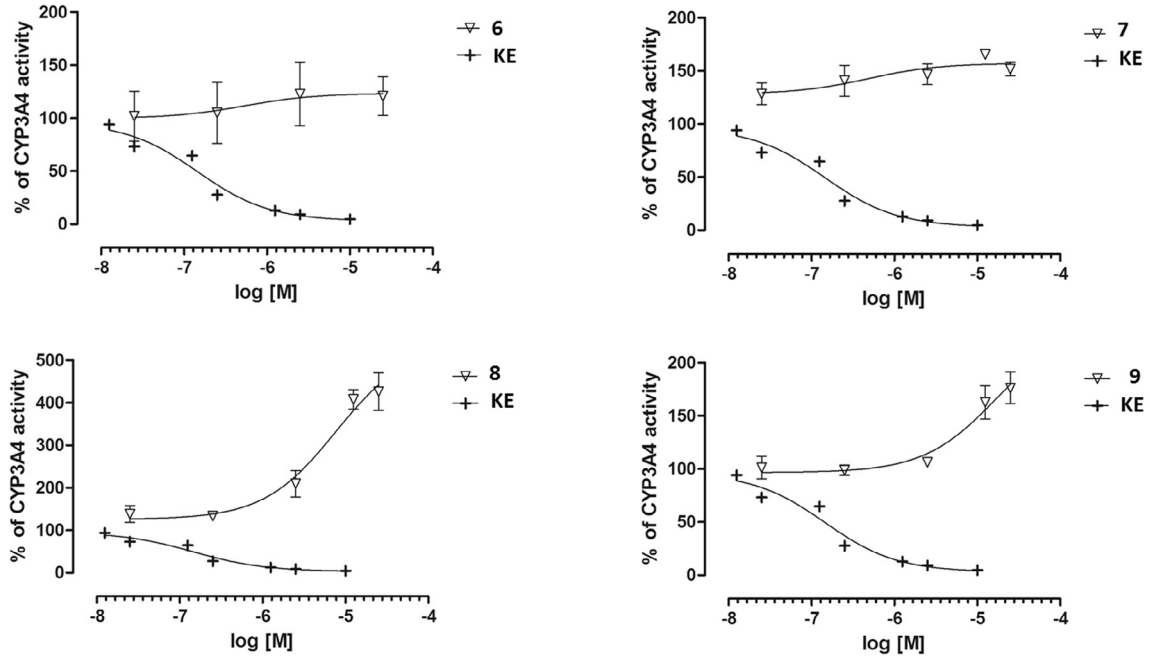

Fig. 10. The effect of **6**, **7**, **8**, **9** (0.025 μM–25 μM) and ketoconazole (0.010 μM–10 μM) on CYP3A4 activity.

ence on cytochrome CYP3A4 activity) drug-like properties. Paying attention to described herein ligands' biological activity and docking results, further directions of research include modification of the "eastern part" of the molecule (e.g. introduction of bulky aromatic groups: naphthyl, biphenyl) in order to test, whether larger substituents are also tolerated.

4. Experimental

4.1. Chemistry

All reagents were purchased from commercial suppliers and were used without further purification. 3-methyl piperidine was used as racemate, and the stereochemistry of its' final derivatives (**3**, **7**, **11**, **15**, **19**) were therefore not determined. Melting points (m.p.) were determined on a MEL-TEMP II (LD Inc., USA) melting point apparatus and are uncorrected. IR spectra were measured as KBr pellets on FT Jasco IR spectrometer. UV spectra were recorded on a Jasco UV/Vis V-530 apparatus in 10^{-5} mol/L in methanol. Mass spectra (LC/MS) were performed on Waters TQ Detector mass spectrometer. ^{1}H NMR spectra were recorded on a Varian Mercury 300 MHz PFG spectrometer in DMSO-d_6 or in $CDCl_3$. Chemical shifts were expressed in parts per million (ppm) using the solvent signal as an internal standard. Data are reported in the following order: multiplicity (s, singlet; d, dublet; t, triplet; qi quintet, m, multiplet; br, broad; *t*-p, *tert-pentyl*; Ph, phenyl; Pip, piperidine, Azp, azepane), approximate coupling constants *J* expressed in Hertz (Hz), number of protons. ^{13}C NMR spectra were recorded on Varian-Mercury-VX 300 MHz PFG or Brukker 400 MHz spectrometer at 75 MHz in DMSO-d_6. LC–MS were carried out on a system consisting of a Waters Acquity UPLC, coupled to a Waters TQD mass spectrometer. Retention times (t_R) are given in minutes. The UPLC/MS purity of all final compounds was determined (%). Elemental analyses (C, H, N) were performed on an Elemental AnalyserVario El III (Hanau, Germany) and agreed with theoretical values within ±0.4%. TLC data were obtained with Merck silica gel 60F_{254} aluminum sheets with the following detection with UV light and evaluation with Dragendorff's reagent (solvent system: methylene chloride: methanol 9:1). RP-TLC data were obtained with Merck Silica gel 60 RP-18 F_{254}S glass plates, using planar chromatographic CHROMDES chambers. Compounds solutions were applied using Hamilton 25 μl syringes. The following detection was obtained by evaluation in iod-saturated glass chambers. For CC (column chromatography using silica gel 60 (0.063–0.20 mm; Merck) solvent systems were used: I-CH_2Cl_2; II: CH_2Cl_2:MeOH (9:1).

4.1.1. General procedure (a) for compounds ***1a–1e***

Starting compounds were obtained according the procedure described in Ref. 22. Analytical data of compounds **1a**–**1e** could be found in Ref. 20. Detailed synthetic procedure for compounds **1b**–**1e** could be found in Appendix A: Supplementary Data.

A solution of freshly prepared sodium propylate, proper substituted phenols were added and stirred in room temperature for 15 min. α,ω-dibromoalkanes were then added drop wisely in the time of 1 h. The reaction mixture was stirred in 60 °C for 3 h, and then refluxed for another 3 h. After cooling down to RT mixture was filtrated and evaporated. To a rough product, 100 ml of 10% NaOH was added and left overnight in cold. To a resulting white oil CH_2Cl_2 was added, mixed and layers were then separated. Organic layer was dried over sodium sulphate filtered and evaporated. Rough product was used for further reactions without purification.

*4.1.1.1. 1-((4-Bromobutyl)oxy)-4-(tert-pentyl)benzene (**1a**).* Synthesis from *tert*-pentylphenol (16.42 g, 0.1 mol), 1,4-dibromobutane (g, 0.2 mol) in sodium propylate (0.1 mol, 100 ml). Obtained 27 g of raw product, purified by CC (II). Yield 78%.

4.1.2. General synthetic procedure for compounds ***2–21***

To a suspension of potassium carbonate and catalytic amount of potassium iodide in water, a mixture of proper cyclic amine and compound **1a**–**1e** in ethanol was added. Mixture was then refluxed for 8–20 h (TLC controlled). After cooling down to room temperature, reaction mixture was filtrated, evaporated and purified by one of the procedures:

Procedure A: To a resulting oil, 100 ml of CH_2Cl_2 was added and washed with: 0.5% HCl solution, 0.5% NaOH solution and water.

After drying over anhydrous Na_2SO_4 and evaporation of organic layer product was further purified using CC (CH_2Cl_2:MeOH).

Procedure B: To a resulting oil 100 ml of CH_2Cl_2 was added and washed with: 0.5% HCl solution. After drying over anhydrous Na_2SO_4 and evaporation of organic layer, product was suspended in 50 ml of 3% HCl solution and washed with diethyl ether. Organic layer was then alkalized and extracted to CH_2Cl_2.

Resulting oils were transformed into hydrogen oxalates, using 10% excess of oxalic acid ethanol solution in room temperature, and then precipitated by addition of ethyl ether.

Detailed synthetic procedure and analytical data for compounds **2**–**21** could be found in Appendix A: Supplementary Data.

*4.1.2.1. 1-(4-(4-(tert-Pentyl)phenoxy)butyl)piperidine hydrogen oxalate (**2**).* Synthesis from piperidine (0.85 g, 10 mmol), and compound **1a** (1.5 g, 5 mmol) in ethanol (105 ml) in the presence of K_2CO_3 (2.07 g, 15 mmol) and catalytic amount KI in water (20 ml). Refluxed for 20 h. Purified by Procedure **A**, CC eluent: CH_2Cl_2:MeOH (9:1). Obtained 0.75 g of oil. Yield 35%. Raw product was transformed into oxalic acid salt yielding 0.63 g of final compound. Mp: 133–135 °C. R_f = 0.28. ^{1}H NMR (DMSO-d_6) δ: 7.22–7.17 (d, *J* = 8.7 Hz, 2H, Ph-3,5-*H*), 6.85–6.80(d, *J* = 8.7 Hz, 2H, Ph-2,6-*H*), 3.95–3.92 (t, *J* = 6.2 Hz, 2H, C*H*$_2$-O), 3.03–2.98(m, 6H, Pip-2,6-C*H*$_2$ + N-C*H*$_2$), 1.80–1.60 (m, 8H, 3× C*H*$_2$ + *t*-p-C*H*$_2$), 1.59–1.51(m, 4H, 2× C*H*$_2$), 1,18 (s, 6H, 2× C*H*$_3$), 0.61–0.56(t, *J* = 7.3 Hz, 3H, CH_2-C*H*$_3$). ^{13}C NMR (DMSO-d_6)™: 165.11, 156.61, 141.27, 127.13, 114.35, 67.14, 56.11, 52.43, 37.36, 36.72, 28.92, 26.52, 23.00, 21.98, 20.78, 9.51;UV–VIS λ [nm] (lgε): 216 (3.89), 223 (3.89), 276 (3.78), 282 (3.71). IR (cm^{-1}): 3429.78 (N(CH_2–)$_4$), 3022.87 (aromatic CH═), 2961.16 (het. CH_2–), 2875.34, 2679.60, 2537.86, 2365.26, 1719.23, 1700.91, 1608.34, 1579.41, 1491.67, 1475.28, 1384.64, 1362.46, 1294.97 (O–CH aromatic), 1186.01, 1115.62, 1034.62, 993.16, 953.63, 831.17, 779.10, 704.85 (alif. CH_2–), 662.43, 521.65. LC–MS: purity 100% t_R = 5.90, (ESI) *m*/*z* [M +H]$^+$ 304.24. Anal. Calcd for $C_{20}H_{33}NO \times C_2H_2O_4$: C, 67.14, N, 3.56, H, 8.96%. Found: C, 67.22, N, 3.61, H, 9.25.

4.2. Lipophilicity

Lipophilicity, by means of R_{M0} values, was estimated using RP-TLC planar method. Methanol:acetic acid:water (with constant, 10% acid concentration) solvent mixture was used as a mobile phase. Organic solvent concentration varied from 85% to 55%, by 5% each step. Mobile phase composition as well as concentrations were chosen experimentally. For each concentration, 10 μl of compounds methanol solution in 1 mg/ml concentration was used. Planar chromatographic chambers (Chromdes) were saturated with proper mixture for 45 min. followed by 15 min. saturation together with the plate. Glass plates (Merck RP-18, FP_{254}s) were then evaluated on the distance of 90 mm, dried and spots were visualized using iod fumes. For each of the compounds, on the base of R_f values, R_M values were determined. R_{M0} values were read from R_M/methanol concentration charts, after extrapolation to zero methanol concentration using in-house script.

4.3. X-ray structure analysis

Crystal data for **18**: C_{24} H_{42} N O, C_2 H_2 O_4, M = 449.61, triclinic, space group *P*1, a = 8.4543(2) Å, b = 11.1330(3) Å, c = 14.7601 (11) Å, 〈 = 89.363(1) (°), ® = 84.8700(9) (°), © = 73.511(6) (°), V = 1326.63(12) Å^3, Z = 2, D_x = 1.126 g cm^{-3}, T = 296 K, μ = 0.612 mm^{-1}, λ = 0.71073 Å, data/parameters = 3703/559; final R_1 = 0.06.

Crystallographic data (excluding structural factors) for the structure reported in this paper has been deposited at the Cambridge Crystallographic Data Centre and allocated with the deposition number CCDC 1485473. Copies of the data can be obtained free of charge on application to CCDC, 12 Union Road, CambridgeCB2 1EW, UK (Fax: Int code +(1223)336-033; E-mail: deposit@ccdc.cam.ac.uk).

4.4. Docking studies

In silico visualization of binding to histamine H_3R model described by Levoin et al., was held using Glide module of Schrödinger MacroModel 10.5.[43–46] All of the tested compounds were used in their *N*-protonated form, and generated using Schrödinger suite, despite compound **18** where crystallographic structure was used for docking. For the tested compounds energetically optimal conformers were found using ConfGen (MMFFs forcefield, PRCG, convergence threshold = 0.05, 20 steps per rotatable bond, max. ring conformations = 16). For all of the structures 5 energetically best conformations were used for docking.

Receptor grid was generated by GlideGrid module and validated with previously described BP.294 (Pitolisant). Docking studies were performed via GlideDock module (OPLS 2001 forcefield, solvent = water, standard precision, post-docking minimization). Results were interpreted by the means of Docking Score functions.

Receptor-ligand interactions were visualized using PyMOLver 1.4.1.[47]

4.5. Pharmacology

4.5.1. General remarks

Competition binding data were analyzed by the GraphPad-PrismTM (200, version 3.02, San Diego, CA, USA) software, using non-linear least squares fit. Affinity values (K_i) were expressed as mean from at least two experiments in triplicates with SEM. K_i values were calculated from IC_{50} values according to Cheng-Prusoff equation.[48]

4.5.2. [^{125}I]Iodoproxyfan hH_3R displacement assay

The displacement binding assay was carried out as described by Ligneau et al.[23] In brief, membrane preparations of CHO-K1 cells expressing the recombinant hH_3R gene were homogenized, incubated for 90 min at 25 °C and shook at 250 rpm with [^{125}I] Iodoproxyfan (16–50 pM) and different concentrations of the test compound. Non-specific binding was determined in the presence of imetit (1 μM). In saturation binding experiments B_{max} was found to be 0.6 pmol/mg and the K_d value was 0.044 pM. The bound radioligand was separated from free radioligand by filtration through GF/B filters (pre-treated with 0.3% (m/v) polyethyleneimine using an Inotech cell harvester Dottikin, Switzerland). Unbound radioligand was removed by four washing steps with 5 ml/well of binding buffer.

4.5.3. [^{3}H]N^α-Methylhistamine hH_3R displacement assay

The displacement binding assay was carried out as described by Kottke et al.[24] Frozen crude membrane preparations of HEK-293 cells stably expressing the recombinant hH_3R in full length were thawed, homogenized, incubated for 90 min at 25 °C and shook at 250 rpm with [^{3}H]N^α-methylhistamine (2 nM) and different concentrations of the test compounds (seven appropriate concentrations between 0.01 nM and 10 μM were used) in a final assay volume of 200 μl per well. Non-specific binding was determined in the presence of *Pitolisant* (10 μM). In saturation binding experiments B_{max} was found to be 0.89 pmol/mg and the K_d value of [^{3}H] N^α-methylhistamine was 2.98 nM. The bound radioligand was separated from free radioligand by filtration through GF/B filters (pre-treated with 0.3% (m/v) polyethyleneimine) using an Inotech cell harvester (Dottikin, Switzerland). Unbound radioligand was removed by three washing steps with 0.3 ml/well of ice-cold

50 mM Tris-HCl buffer (pH 7.4) containing 120 mM NaCl. Scintillation cocktail was added and the liquid scintillation counting was performed with a Perkin Elmer TriluxBetacounter (Perkin Elmer, Germany).

4.5.4. cAMP accumulation assay in cells expressing hH_3R

Intracellular cAMP accumulation was measured with homogenous TR-FRET immunoassay, using LANCE *Ultrac*AMP kit (PerkinElmer) and HEK293 cells, stably expressing hH_3R. An antagonist dose-response experiments were performed in a total assay volume of 20 μl in white 384-well plates, using 300 cells/well. (R)(−)-α-Methylhistamine (15 nM), forskolin (10 μM) and antagonists in appropriate concentrations (in range 0.1 nM–10 μM) were added simultaneously to cell suspension. Cells stimulation was performed for 30 min at room temperature. After incubation period, five microliters of europium (Eu) chelate-labeled cAMP tracer and 5 μl of U*Light*-labeled *anti*-cAMPmAb working solutions were added, mixed and incubated for 1 h. TR-FRET signal was read on an EnSpire microplate reader (PerkinElmer). Measured TR-FRET signal was translated into actual quantities of produced cAMP on the basis of cAMP standard curve and obtained results were presented as% of maximal response. Sigmoidal dose-response curve fitting was performed with use of GraphPad Prism™ software (version 5.01, San Diego, CA, USA). Showed results represent the mean of three separate experiments, each performed in triplicates.

4.6. In vivo studies

4.6.1. Anticonvulsant screening program

Anticonvulsant evaluation of compounds was performed and sponsored by National Institute of Neurological Disorders and Stroke, National Institutes of HealthCountry name of "National Institutes of Health" is "United States". (Rockville, USA) for the Anticonvulsant Screening Program (ASP). Compounds were injected as suspensions in 0.5% methylcellulose at the selected doses (30, 100 or/and 300 mg/kg). As experimental animals male albino mice (CF-1 strain) and male albino rats (Sprague-Dawley) were used. Observations were carried out after 0.5 h and 4 h after administration. Groups of eight mice or four rats were employed. Phase 1 of ASP includes three tests performed in mice (i.p.): maximal electroshock (MES), subcutaneous pentylenetetrazole (scMET), and neurotoxicity (rotarod test). Selected compounds were administered orally into rats using four animals at a fixed dose of 30 mg/kg (MES test) (Phase VIa).

4.6.1.1. Maximal electroshock seizure test (MES) test. Seizures were elicited by 60 Hz alternating current (50 mA in mice) delivered for 2 s by corneal electrodes. A drop of 0.5% tetracaine HCl in 0.9% NaCl solution was placed into each eye prior to applying electrodes. Protection was defined as abolition of the hindlimb tonic extension component of the seizure.[49,50]

4.6.1.2. Subcutaneous pentetrazole induced seizures. A dose of pentetrazole which induce convulsions in 97% of animals (CD97: 85 mg/kg mice) was injected into a loose fold of skin in the midline of the neck. Animals were observed for 30 min for the presence or absence of a seizure. Failure of observing even a threshold seizure (a single episode of clonic spasm which remains at least 5 s) was classified as protection.[27]

4.6.1.3. Neurotoxicity test. The rotarod test was used to evaluate neurotoxicity in rodents (mice). Animal was placed on a 1 in. diameter knurled plastic rod rotating at 6 rpm. The animal can maintain its equilibrium for long periods of time. Neurotoxicity was indicated if animal falls off this rotating rod three times during a 1-min period.[51]

4.7. Antiproliferative assay

4.7.1. Cell lines

Neuroblastoma IMR-32 cell line was provided by Department of Oncogenomics, AcademischMedisch Centrum, Amsterdam, Holland.[52,53] Human embryonic kidney HEK-293 cell line (ATCC CRL-1573) was kindly donated by Prof. Dr. Christa Müller (Pharmaceutical Institute, Pharmaceutical Chemistry I, University of Bonn).

4.7.2. In vitro antiproliferative assay

DMEM cell culture medium (Gibco) with 10% fetal bovine serum (FBS), 100 mg mL^{-1} streptomycin and 100 U mL^{-1} penicillin was used for both cell lines. The cells were seeded in 96-well plates at a concentration of 2×10^4 cells/well (IMR-32) or 1.5×10^4 cells/well (HEK-293) in 200 μl culture medium and incubated for 24 h at 37 °C and 5% $CO_2$to reach 60% confluence. The stock solutions of H_3 receptor ligands in DMSO (25 mM) were diluted into fresh growth medium to the final concentrations 0.01 μM–250 μM and added to the culture. The DMSO concentration did not exceed 1%. After 48 h of incubation, the 20 μl ofEZ4U (EZ4U Non-radioactive cell proliferation and cytotoxicity assay, Biomedica) labeling mixture was added to each well and the cells were next incubated for 5 h. The absorbance of the samples was measured using a microplate reader (PerkinElmer) at 492 nm. The activity of the standard drug doxorubicin (DX) was estimated as we described previously.[36]

4.8. Metabolic stability

4.8.1. Reaction with recombinant human liver microsomes (HLM)

Commercial, pooled, human (adult male & female) liver microsomes (HLMs) from Sigma-Aldrich were used for all biotransformations. The reaction was carried out using 1 mg/ml HLMs in 200 μl of reaction buffer containing 0.1 M Tris-HCl (pH 7.4), NADPH Regeneration System (Promega) and H_3 receptor ligand with final volume of 50 μM at 37° for 2 h. The reaction was initiated by adding 50 μl of Regeneration System after 5 min. preincubation at 37 °C. The 200 μl of cold methanol was added to terminate the reaction. The mixture was centrifuged at 13,000 rpm for 15 min. and then LC/MS analysis of the supernatant was performed. Mass spectra were recorded on LC/MS system consisted of a Waters Acquity UPLC, coupled to a Waters TQD mass spectrometer (electrospray ionization mode ESI-tandem quadrupole).

4.8.2. CYP3A4 P450-Glo™ assay

The CYP3A4 inhibitor ketoconazole was purchased from Sigma-Aldrich. The enzymatic reactions were performed in white polystyrene, flat-bottom Nunc™ MicroWell™ 96-Well Microplates (Thermo Scientific). The luminescence signal was measured with a microplate reader in luminescence mode (PerkinElmer). The CYP3A4 P450-Glo™ assay and protocol were provided by Promega.[41] The IC_{50} value of the reference compound ketoconazole was determinate and calculated as we described previously.[42] The final concentrations of H_3R ligands were 0.025 μM–25 μM and the CYP3A4 inhibitor ketoconazole 0.010 μM–10 μM.

4.8.3. In silico study

The metabolic biotransformation of H_3R ligands was studied *in silico* by using computational software MetaSite 4.1.1 provided by Molecular Discovery Ltd (2013)[54,55] using liver model.

Acknowledgements

We grateful thank Senior scientist Mohamed Hamdi from Department of Oncogenomics Academisch Medisch Centrum

Amsterdam, Holland for providing neuroblastoma IMR-32 cell line. We would like to thank prof. James P. Stables, prof. Jeff Jiang and Tracy Chen, Ph.D. for providing the results of anticonvulsant assays through ASP at National Institute of Neurological Disorders and Stroke, National Institutes of Health (Rockville, USA).We are pleased to acknowledge the generous support of National Science Center, Poland granted on the basis of decision No. DEC-2011/02/A/NZ4/00031 and K/ZDS/004689 and of the European COST Action GLISTEN-CM1207.

Supplementary data

Supplementary data associated with this article can be found, in the online version, at http://dx.doi.org/10.1016/j.bmc.2017.03.031. These data include MOL files and InChiKeys of the most important compounds described in this article.

References

1. Parsons ME, Ganellin CR. Histamine and its receptors. *Br J Pharm*. 2006;147 (Suppl. 1):S127–S135.
2. Tiligada E, Kyriakidis K, Chazot PL, Passani MB. Histamine pharmacology and new CNS drug targets. *CNS Neurosci Ther*. 2011;17:620–628.
3. Walter M, Stark H. Histamine receptor subtypes: a century of rational drug design. *Front Biol Sci*. 2012;461–488.
4. Schlicker E, Kathmann N. Modulation of in vitro neurotransmission in the CNS and in the retina via H3 receptors. In: Leurs R, Timmerman H, eds. *The Histamine H3 Receptor. A Target For New Drugs*. Elsevier; 1998.
5. Blandina P, Bacciottini L, Giovannini MG, Mannaioni PF. H3 receptor modulation of the release of neurotransmitters in vivo. In: Leurs R, Timmerman H, eds. *The Histamine H3 Receptor. A Target for New Drugs*. Elsevier; 1998:27–40.
6. Tiligada E, Zampelli E, Sander K, Stark H. Histamine H_3 and H_4 receptors as novel drug targets. *Expert Opin Investig Drugs*. 2009;18:1519–1531.
7. Berlin M, Boyce CW, de Lera Ruiz M. Histamine H_3 receptor as a drug discovery target. *J Med Chem*. 2011;5426–5453.
8. Incerti M, Flammini L, Saccani F, et al. Dual-acting drugs: an in vitro study of nonimidazole histamine H_3 receptor antagonists combining anticholinesterase activity. *ChemMedChem*. 2010;5:1143–1149.
9. Pala D, Scalvini L, Lodola A, et al. Synthesis and characterization of new bivalent agents as melatonin-and histamine H_3-ligands. *Int J Mol Sci*. 2014;15:16114–16133.
10. Khanfar MA, Affini A, Lutsnko K, Nikolic K, Butini S, Stark H. Multiple targeting approaches on histamine H_3 receptor antagonists. *Front Neurosci*. 2016;10:1–17.
11. Jadhav HR, Singh M. Histamine H_3 receptor function and ligands: recent developments. *Mini-Rev Med Chem*. 2013;13:47–57.
12. Łażewska D, Kieć-Kononowicz K. New developments around histamine H_3 receptor antagonist/inverse agonists: a patent review (2010-present). *Exp Opin Ther Pat*. 2014;24:89–111.
13. Schwartz JC. The histamine H_3 receptor: from discovery to clinical trials with pitolisant. *Br J Pharm*. 2011;163:713–721.
14. European Medicines Agency. <http://www.ema.europa.eu> Accessed 06.12.2016.
15. Sander K, Kottke T, Hoffend C, et al. First metal-containing histamine H_3 receptor ligands. *Org Lett*. 2010;12:2578–2581.
16. Wingen K, Stark H. Scaffold variations in amine warhead of histamine H_3 receptor antagonists. *Drug Discovery Today Technol*. 2013;4:483–489.
17. Cowart M, Hsieh G, Black LA, et al. Pharmacological characterization of A-960656, a histamine H_3 receptor antagonist with efficacy in animal models of osteoarthritis and neuropathic pain. *Eur J Pharmacol*. 2012;684:87–94.
18. Bakker RA. Histamine H_3-receptor isoforms. *Inflamm Res*. 2004;53:509–516.
19. Łażewska D, Ligneau X, Schwartz JC, Schunack W, Stark H, Kieć-Kononowicz K. Ether derivatives of 3-piperidinopropan-1-ol as non-imidazole histamine H_3 receptor antagonists. *Bioorg Med Chem*. 2006;14:3522–3529.
20. Sadek B, Kuder K, Subramanian D, et al. Anticonvulsive effect of nonimidazole histamine H_3 receptor antagonists. *Behav Pharmacol*. 2014;25:245–252.
21. Alter A. Disubstituted piperazines useful as schistosomiasis agents. US3270004; 1966.
22. Kuder K, Łażewska D, Latacz G, et al. Chlorphenoxy aminoalkyl derivatives as histamine H_3R ligands and antiseizure agents. *Bioorg Med Chem*. 2016;24:53–72.
23. Ligneau X, Morisset S, Tardivel-Lacombe J, et al. Distinct pharmacology of rat and human histamine H(3) receptors: role of two amino acids in the third transmembrane domain. *Br J Pharmacol*. 2000;131:1247–1250.
24. Kottke T, Sander K, Weizel L, Schneider EH, Seifert S, Stark H. Receptor-specific functional efficacies of alkyl imidazoles as dual histamine H_3/H_4 receptor ligands. *Eur J Pharmacol*. 2011;654:200–208.
25. Lipp R, Stark H, Schunack W. Receptor biochemistry and methodology. In: Schwartz J-C, Haas HL, eds. *The Third Histamine Receptor*. New York: Wiley Liss; 1992:57–72.
26. Ganellin CR, Leurquin F, Piripitsi A, et al. Synthesis of potent non-imidazole histamine H_3-receptor antagonists. *Arch Pharm*. 1998;331:395–404.
27. Stables JP, Kupferberg HJ. In: Avanzin G, Regesta G, Tanganelli P, Avoli M, eds. *Molecular and Cellular Targets for Antiepileptic Drugs*. London: John Libbey & Company Ltd; 1997:191–198. 23129.
28. White SH, Woodhead JH, Wilcox KS, Stables JP, Kupferberg HJ, Wolf HH. In: Levy RH, Mattson RH, Meldurm BS, Perucca E, eds. *Antiepileptic Drugs*. 5th ed. Philadelphia: Lippincott Williams & Wilkins; 2002:36–48.
29. Biagi GL, Barbaro AM, Sapone A, Recanatini M. Determination of lipophilicity by means of reversed-phase thin-layer chromatography I. Basic aspects and relationship between slope and intercept of TLC equations. *J Chromatogr*. 1994;662:341–361.
30. CambridgeSoft, Cambridge. *ChemBio3D, 11.0, Demo Version*, 2010.
31. ChemAxon Kft. *Marvin Beans 14.9.22.0, Demo Version*, 2014.
32. *Schrödinger Release 2016-01; Maestro, Version 10.5*. New York, NY: Schrödinger LLC; 2016.
33. GPCRM Structure Modelling Server. <http://gpcrm.biomodellab.eu/> Accessed 04.07.2016.
34. Levoin N, Calmels T, Poupardin-Olivier O, et al. Refined docking as a valuable tool for lead optimization: application to histamine H_3 receptor antagonists. *Arch Pharm Chem Life Sci*. 2008;341:610–623.
35. Bajda M, Kuder KJ, Łażewska D, et al. Dual-acting diether derivatives of piperidine and homopiperidine with histamine H_3 receptor antagonistic and anticholinesterase activity. *Arch Pharm Chem Life Sci*. 2012;345:591–597.
36. Schlegel B, Laggner C, Meier R, et al. Generation of a homology model of the human histamine H3 receptor for ligand docking and pharmacophore-based screening. *J Comput Aided Mol Des*. 2007;21:437–453.
37. Kerns EH, Di L. *Drug-like Properties: Concepts, Structure Design and Methods*. Burlington, MA: Academic Press; 2008.
38. Grosicki M, Latacz G, Szopa A, Cukier A, Kieć-Kononowicz K. The study of cellular cytotoxicity of argireline (R) – an anti-aging peptide. *Acta Biochim Pol*. 2014;61:29–32.
39. Natang AS, Desai DS. *Anticancer drug development. Pharmaceutical perspectives of cancer therapeutics*. US: Springer; 2009.
40. Cruciani G, Carosati E, De Boeck B, et al. MetaSite: understanding metabolism in human cytochromes from the perspective of the chemist. *J Med Chem*. 2005;48:6970–6979.
41. Cali JJ, Ma D, Sobol M, et al. Luminogenic cytochrome P450 assays. *Expert Opin Drug Metab Toxicol*. 2006;2:629–645.
42. Łażewska D, Więcek M, Ner J, et al. Aryl-1,3,5-triazine derivatives as histamine H4 receptor ligands. *Eur J Med Chem*. 2014;18:534–546.
43. *Schrödinger Release 2016-4: Glide*. New York, NY: Schrödinger, LLC; 2016.
44. Friesner RA, Murphy RB, Repasky MP, et al. Extra precision glide: docking and scoring incorporating a model of hydrophobic enclosure for protein-ligand complexes. *J Med Chem*. 2006;49:6177–6196.
45. Halgren TA, Murphy RB, Friesner RA, et al. Glide: a new approach for rapid, accurate docking and scoring. 2. Enrichment factors in database screening. *J Med Chem*. 2004;47:1750–1759.
46. Friesner RA, Banks JL, Murphy RB, et al. Glide: a new approach for rapid, accurate docking and scoring. 1. Method and assessment of docking accuracy. *J Med Chem*. 2004;47:1739–1749.
47. PyMOL(TM). Version 1.4.1. Schrodinger LLC.
48. Cheng Y, Prusoff WH. Relationship between the inhibition constant (K_i) and the concentration of inhibitor which causes 50 per cent inhibition (I_{50}) of an enzymatic reaction. *Biochem Pharmacol*. 1973;22:3099–3108.
49. Swinyard EA, Woodhead JH, White HS, Franklin MR. General principles: experimental selection, quantification, and evaluation of anticonvulsants. In: Levy RH, Mattson RH, Melrum B, Penry JK, Dreifuss FE, eds. *Antiepileptic Drugs*. 3rd ed. New York: Raven Press; 1989:85–102.
50. White HS, Woodhead JH, Franklin MR. General principles: experimental selection, quantification, and evaluation of antiepileptic drugs. In: Levy RH, Mattson RH, Melrum B, Penry JK, Dreifuss FE, eds. *Antiepileptic Drugs*. 3rd ed. New York: Raven Press; 1989:99–110.
51. Dunham MS, Miya TA. A note on a simple apparatus for detecting neurological deficit in rats and mice. *J Am Pharm Ass Sci*. 1957;46. 208–207.
52. Cheng NC, Van Roy N, Chan A, et al. Deletion mapping in neuroblastoma cell lines suggests two distinct tumour suppressor genes in the 1p35-36 region, only one of which is associated with N-myc amplification. *Oncogene*. 1995;10:291–297.
53. Tumilowicz JJ, Nichols WW, Cholon JJ, Greene AE. Definition of a continuous human cell line derived from neuroblastoma. *Cancer Res*. 1970;30:2110–2118.
54. Cruciani G, Carosati E, De Boeck B, et al. Metasite: understanding metabolism in human cytochromes from the perspective of the chemist. *J Med Chem*. 2005;48:6970–6979.
55. Boyer D, Bauman JN, Walker DP, Kapinos B, Karki K, Kalgutkar AS. Utility of MetaSite in improving metabolic stability of the neutral indomethacin amide derivative and selective cyclooxygenase-2 inhibitor 2-(1-(4-chlorobenzoyl)-5-methoxy-2-methyl-1*H*-indol-3-yl)-*N*-phenethyl-acetamide. *Drug Metab Dispos*. 2009;37:999–1008.